Journal of Nepal Geological Society, 2008, Vol. 38, pp. 1–8

Earthquakes and crustal structure of Himalaya from Himalayan Nepal–Tibet seismic experiment (HIMNT)

***Anne F. Sheehan[1], Thomas de la Torre[1], Gaspar Monsalve[1], Vera Schulte-Pelkum[1], Roger Bilham[1], Frederick Blume[1], Rebecca Bendick[1], Francis Wu[2], M. R. Pandey[3], S. Sapkota[3], and S. Rajaure[3]**

[1]*University of Colorado at Boulder, Boulder, Colorado, USA*

[2]*Binghamton University, Binghamton, New York, USA*

[3]*Department of Mines and Geology, National Seismological Centre, Kathmandu, Nepal*

(**Email: afs@cires.colorado.edu)*

ABSTRACT

The Himalayan Nepal–Tibet PASSCAL Seismic Experiment (HIMNT) included the deployment of 28 broadband seismometers throughout eastern Nepal and southern Tibet in 2001–2002. The main goals of the project were to better understand the mountain building processes of this region through studies of seismicity and Earth structure determined from local and teleseismic earthquakes. The seismic deployment was in collaboration with the National Seismological Centre, Department of Mines and Geology, Nepal, and the Institute of Geology and Geophysics of the Chinese Academy of Sciences. Our new subsurface images from HIMNT teleseismic receiver functions and local earthquake tomography show evidence of the basal decollement of the Himalaya (Main Himalayan Thrust, MHT) and an increase in Moho depth from ~45 km beneath Nepal to ~75 km beneath Tibet. We find strong seismic anisotropy above the decollement, likely developed in response to shear on the MHT. The shear may be taken up as slip in great earthquakes at shallower depths. Many local earthquakes were recorded during the deployment, and the large contrast in crustal thickness and velocity structure over a small lateral distance makes the use of a 3D velocity model important to determine accurate hypocentres. Large north-south variations are found in P and S wave velocity structure across the array. High Pn velocities are found beneath southern Tibet. Seismicity shows strong alignment of shallow (15–25 km depth) events beneath the region of highest relief along the Himalayan Front, and a cluster of upper mantle earthquakes beneath southern Tibet (70–90 km depth). Weak-mantle models do not expect the upper mantle earthquakes. Focal mechanisms of these upper mantle earthquakes beneath southern Tibet are mostly strike-slip, markedly different from the normal faulting mechanisms observed for earthquakes in the mid and upper crust beneath Tibet. This change in the orientation of the major horizontal compression axis from vertical in the upper crust to horizontal in the upper mantle suggests a transition from deformation driven by body forces in the crust to plate boundary forces in the upper mantle. Several lines of evidence point to a decoupling zone in the Tibetan mid or lower crust, which may be related to the presence of a previously suggested flow channel in the Tibetan mid crust.

Keywords: Earthquake, crustal structure, Himalaya, Nepal–Tibet seismic experiment

Received: 25 July 2007; **revision accepted:** 8 August 2008

HIMNT DEPLOYMENT

The Himalayan Nepal–Tibet Seismic Experiment (HIMNT) was a USA National Science Foundation (NSF) Incorporated Research Institutions for Seismology (IRIS) Programme for Array Studies of the Continental Lithosphere (PASSCAL) deployment in Nepal and Tibet in 2001–2003 (Fig. 1). HIMNT was the first broadband seismic experiment to simultaneously cover the plains of southern Nepal, the Lesser and Greater Himalaya, and the Southern Tibetan Plateau. The project was led by researchers at the University of Colorado at Boulder (Sheehan, Bilham) and Binghamton University (Francis Wu), in collaboration with the Department of Mines and Geology of Nepal and the Institute of Geology and Geophysics of the Chinese Academy of Sciences. The HIMNT experiment included the deployment of twenty-eight three-component broadband seismic stations, which recorded continuously at a sample rate of 40–50 sps. HIMNT stations were installed with approximately 40–50 km station spacing, covering a two-dimensional area approximately 300 km wide east–west by 300 km north–south. This geometry is well suited for both seismicity and seismic structure projects. Station locations were dictated strongly by logistics. Within each location area, station siting was determined based upon geological conditions, southern exposure for solar panels, and security. In some regions, particularly southern Nepal, bedrock was not available and suitable vaults had to be constructed, which we evaluated in a noise study (de la Torre and Sheehan 2005). The station deployment was executed in several phases. The first phase

included the deployment of seven stations in southern Tibet in August and September of 2001, with 7 more deployed in Tibet in 2002. The second phase of the deployment included 14 stations in eastern Nepal, in October 2001. The fourteen Tibet stations were removed in Autumn 2002. In October and November 2002 five of the Nepal stations were removed, and in April 2003 the remaining ten Nepal stations were removed. The last ten Nepal stations were run collaboratively with the Oregon/Illinois HICLIMB group with data exchanged between our groups.

Each HIMNT station was equipped with Streckeisen STS-2 broadband seismometers, 24-bit Reftek 72A-08 digital data acquisition systems, and GPS clocks from the IRIS PASSCAL instrument pool. Data were recorded continuously using a sample rate of either 40 or 50 samples per second. The data are all archived at the IRIS DMC (data sets YL-2001 and YL-2002 HIMNT Himalayan Nepal Tibet Seismic Experiment) as well as in a local Antelope database.

THREE-DIMENSIONAL SEISMIC VELOCITY STRUCTURE

We used P and S arrival time data from 542 earthquakes recorded by the network in order to simultaneously invert for earthquake location, and P-wave speed (Vp) and P- to S-wave speed ratio (Vp/Vs) for a three dimensional grid of nodes. A total of 5767 P-wave arrivals and 4801 S-wave arrivals were inverted, using a method developed by Thurber (1983,1993) and Eberhart-Phillips (1986), with the program SIMUL2000. The idea is to find the model that minimises the arrival time residuals at the stations. The technique consists of an iterative damped least squares minimisation algorithm. The travel times of the waves between source and receiver are determined by an approximate ray-tracing method (Thurber 1983). Several model parameterisations were tested, using an approach similar to that described by Husen et al. (2000), Eberhart-Phillips (1990) and Eberhart-Phillips and Michael (1998), in which we start solving for velocity structure at coarse grids of nodes, and progressively go to finer ones. The best model parameterisation was chosen based on arrival time misfit and the spread function of the resolution matrix. This function measures how similar the model resolution matrix is to the identity matrix (Menke 1989; Toomey and Foulger 1989; Michelini and McEvilly 1991). The chosen model has a 50 km node spacing in the North–South and East–West directions, and a vertical node separation of around 15 km. Depths go from surface to 70 km below sea level. After inversion, the obtained RMS arrival time residual was 0.31 seconds.

Pandey et al. (1995) identified a concentrated region of microseismicity in the midcrust just to the south of the high Himalaya, which corresponds to regions with high uplift rates (Lave and Avouac 2001). Years of data collected by the National Seismic Centre of the Nepal Department of Mines and Geology have further contributed to the detailed characterisation of seismicity throughout Nepal. Using the HIMNT digital data, we identified 1649 earthquakes between October 2001 and March 2003 by picking P and S arrival times. These earthquakes were relocated using three-dimensional velocity models (Figs. 2 and 3) and the local magnitude was determined using the routine *dbml* from the BRTT Antelope Package. Earthquake local magnitudes range from 1 to 5.5. Earthquakes were relocated using the NonLinLoc software (Lomax 2004), which determines probabilistic, nonlinear earthquake locations in three-dimensional structures. We use the model illustrated in Figs. 2 and 3 in order to relocate the set of 1649 earthquakes. NonLinLoc uses a global optimisation method where for

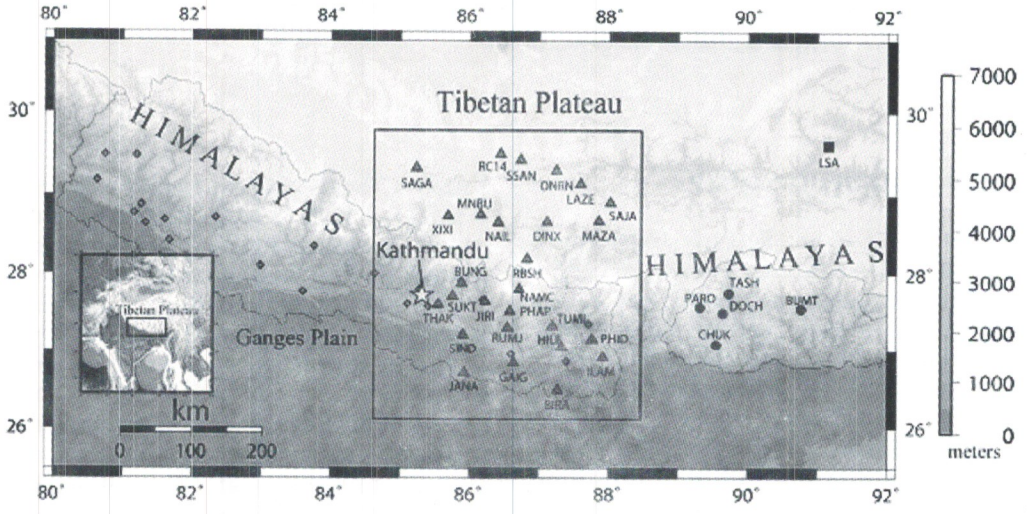

Fig. 1: Grey-scale topography map with HIMNT broadband seismic network (triangles), 2002 Bhutan broadband experiment (circles), Global Seismic Network station LSA (square), and the seismograph stations of the National Seismological Network of Nepal (diamonds).

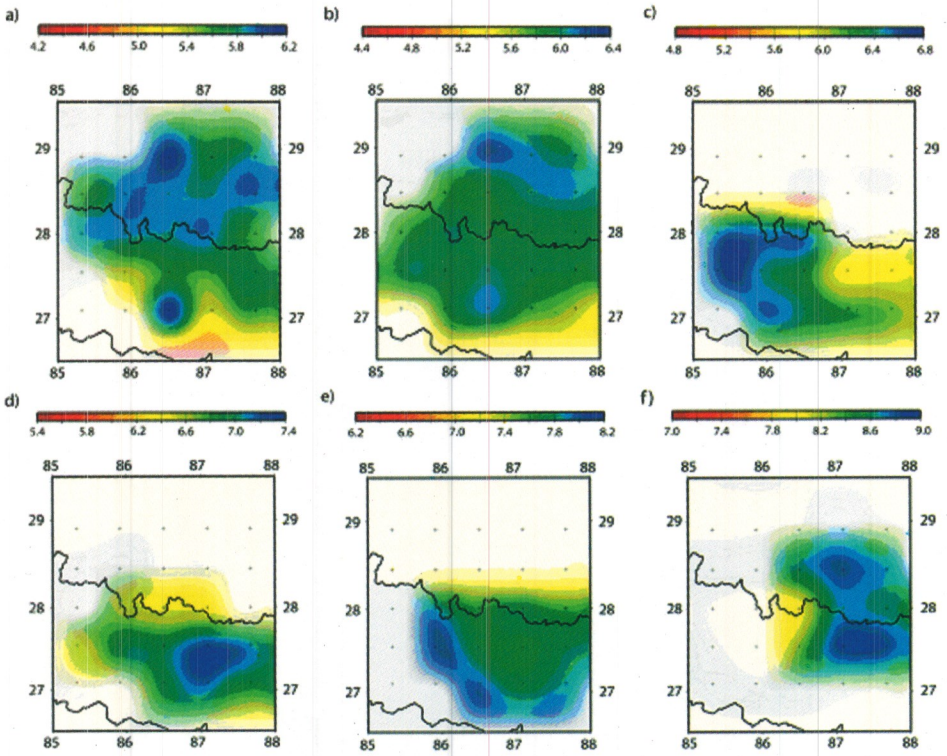

Fig. 2: Three-dimensional P-wave velocity model used for earthquake locations. Horizontal sections of P-wave velocity in km/s at different depths are shown. Only areas with an associated diagonal resolution greater than 0.2 are shown. Vp is mapped at six depths below sea level z : a) z = 3 km, b) z = 15 km, c) z = 25 km, d) z = 40 km, e) z = 55 km, and f) z = 70 km.

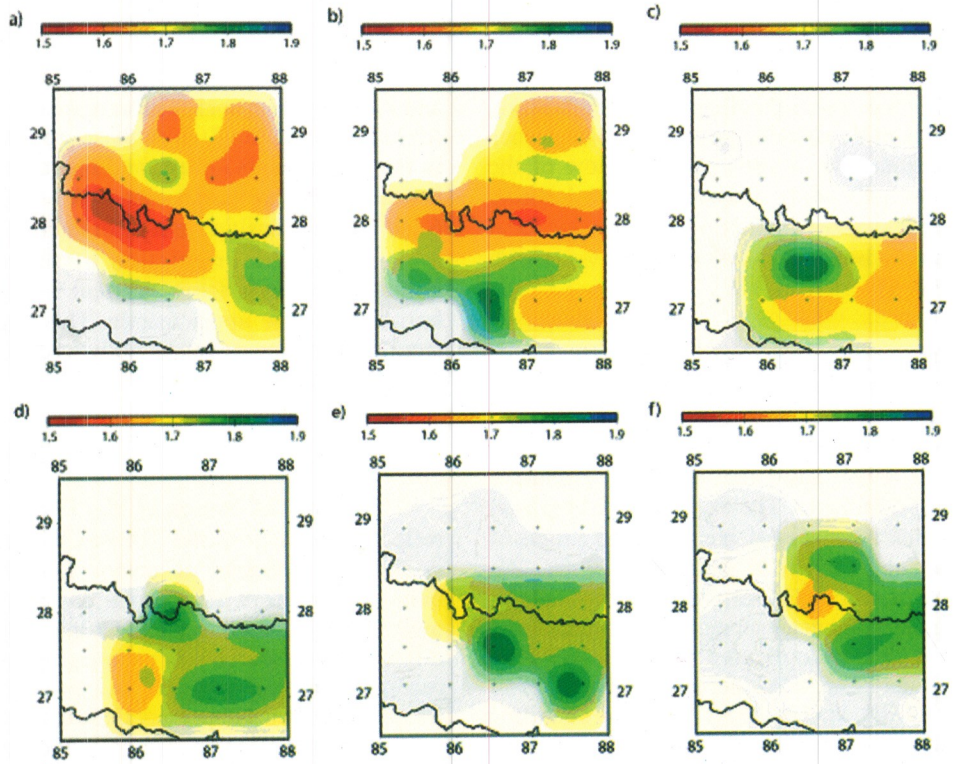

Fig. 3: Horizontal sections of P to S-wave velocity ratios (Vp/Vs) at different depths. Only areas with an associated diagonal resolution greater than 0.2 are shown. Vp/Vs is mapped at six depths below sea level z: a) z = 3 km, b) z = 15 km, c) z = 25 km, d) z = 40 km, e) z = 55 km, and f) z = 70 km.

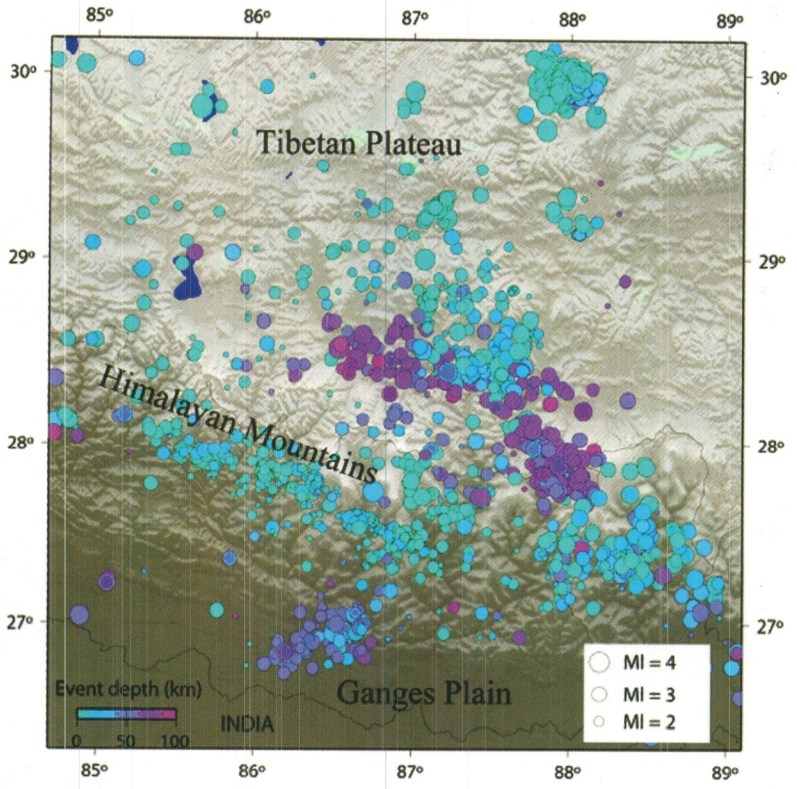

Fig. 4: Map view of HIMNT earthquake locations using the NonLinLoc software. Events are size-scaled by magnitude and colour-scaled by depth.

each set of arrival times corresponding to one earthquake, the whole model space is searched, preventing convergence towards local minima. Fig. 4 shows a map view of the earthquake locations in the study area, with colours denoting hypocentre depth and sizes indicating earthquake local magnitude. A strongly bimodal distribution of events with depth is found (Fig. 5).

MOMENT TENSOR AND SOURCE PARAMETER ANALYSIS

Prior focal mechanism studies (Molnar and Lyon-Caen 1989; Pandey et al. 1995) show that along the Himalaya front thrust faulting dominates. The existence of subcrustal earthquakes, and their mechanisms, has remained a topic of much debate (Chen and Yang 2004; Maggi et al. 2000). We calculated moment tensor inversions for seventeen earthquakes using the moment tensor method of Ammon and Randall (1994) with data collected from the HIMNT experiment, the Bhutan PASSCAL network and the Global Seismic Network (GSN, station LSA). Focal mechanisms were verified with take-off angle and first motion polarities from the broadband data and with seismograms collected from the permanent short period vertical component network of the National Seismic Centre of the Department of Mines and Geology of Nepal. The earthquake focal mechanisms (de la Torre et al. 2007) show that normal faulting is common in the Tibetan upper crust, and that there are many events beneath the Moho, most having strike-slip mechanisms (Figs. 6 and 7). This transition in style of faulting with depth reflects a change in the orientation of the major horizontal compression axis from vertical in the upper crust to horizontal in the upper mantle. This suggests a transition from deformation driven by body forces in the crust to plate boundary forces in the upper mantle.

RECEIVER FUNCTIONS

The model of Nelson et al. (1996), based on seismic reflection data from the Tibetan INDEPTH experiment, implies the existence of several fault bends in the crust beneath the High Himalaya, as suggested in gravity modelling by Lyone-Caen and Molnar (1983), though details differ. Passive-source seismic imaging, such as teleseismic receiver function analysis, can provide complementary images of crust and upper mantle structure. Receiver function analysis of the HIMNT data (Schulte-Pelkum et al. 2005) shows strong Moho converted phases, with Moho depth increasing gradually from 45 km depth beneath Nepal to 75 km beneath the Tibetan Plateau (Fig. 8). A strong anisotropic

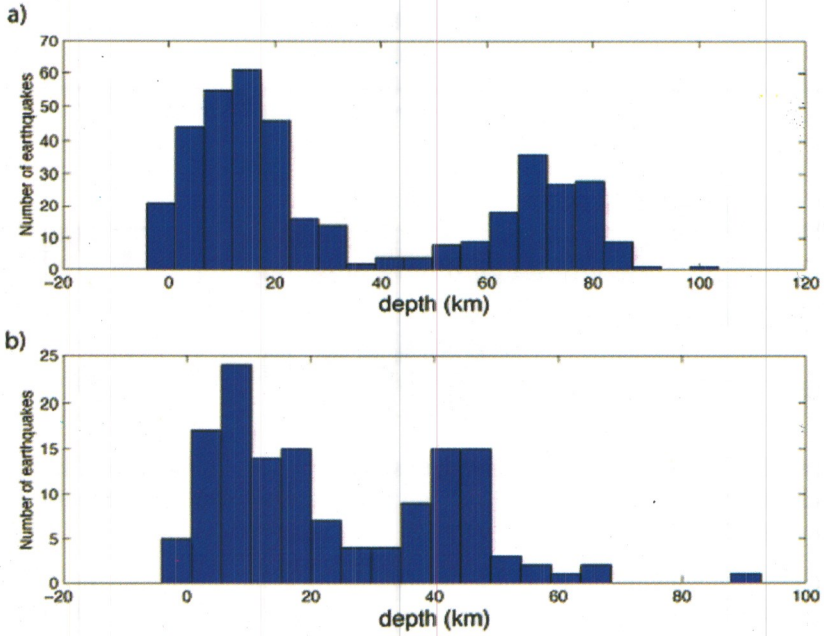

Fig. 5: Histograms of earthquake depth from Monsalve et al. (2006). a) Earthquakes north of 27.5° N. b) Earthquakes south of 27.5° N. Note bimodal distribution of event depth. Histograms were made with the subset of 542 events used to invert for 1-D velocity structure with the program VELEST.

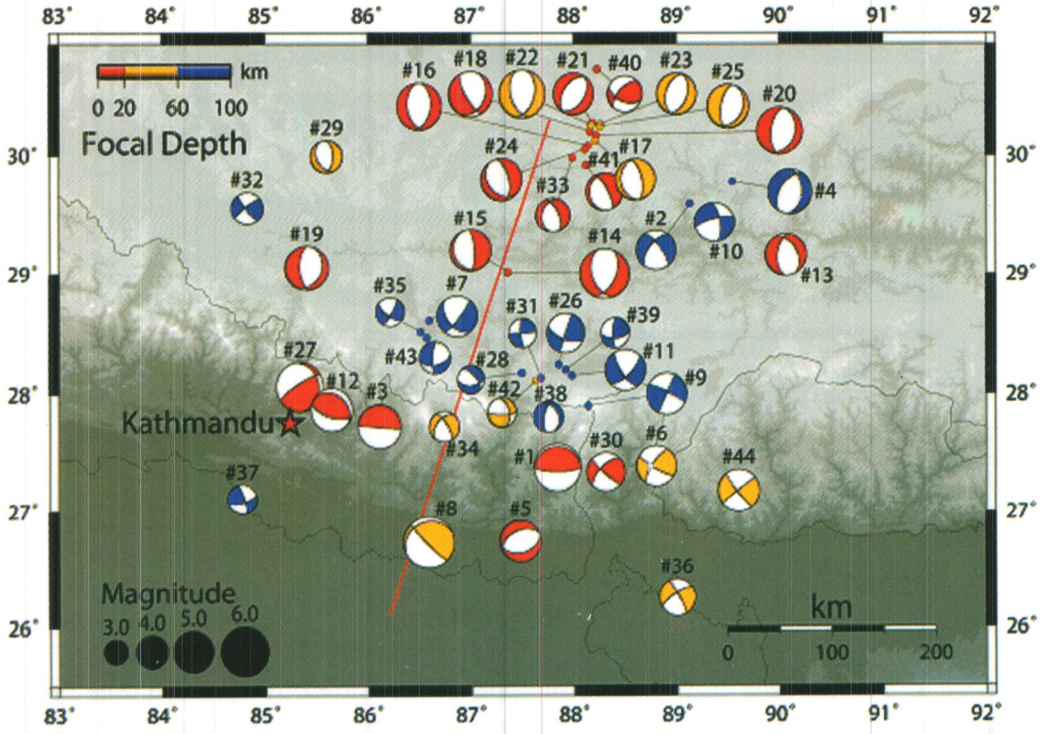

Fig. 6: Focal mechanisms from de la Torre et al. (2007) and other studies. Symbol size scales with magnitude and colour corresponds to event depth.

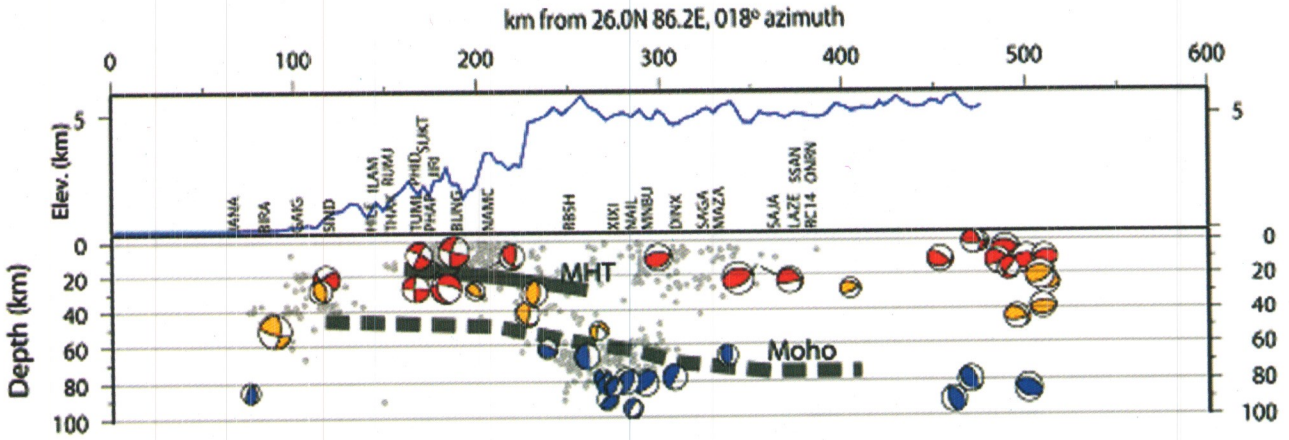

Fig. 7: Cross-section showing seismicity and focal mechanisms. Grey lines denote Main Himalayan Thrust (MHT) and the Moho from Schulte-Pelkum et al. (2005). Regional topography is plotted above the seismicity with approximate locations of the HIMNT stations.

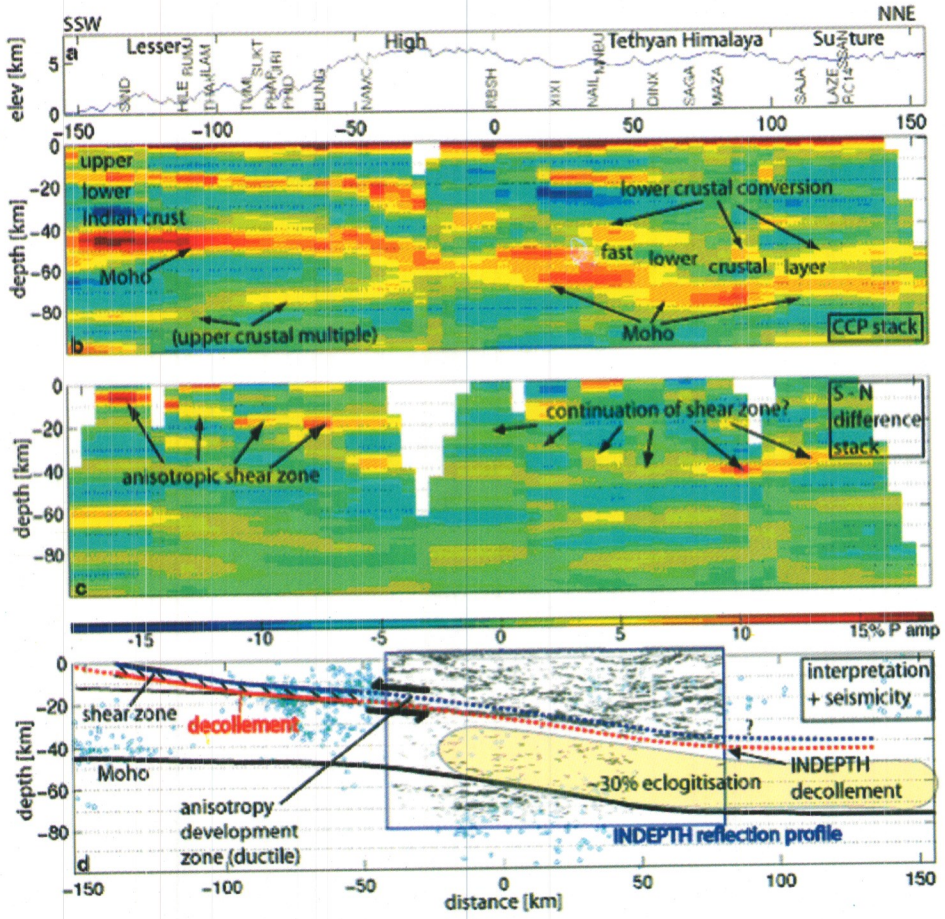

Fig. 8: Results from receiver function analysis and relocation of microseismicity (modified from Schulte-Pelkum et al. 2005). (a) Topography and station locations. (b) Common conversion point (CCP) stack of radial receiver functions. Colour scale is in % of incident P amplitude. Depth migration with 1-D models for Nepal and Tibet from regional tomography. (c) CCP stack of radial receiver functions after north-south differencing, showing a highly anisotropic shear zone (interpreted to be the ductile signature of shear above the decollement in the hanging wall of the Himalaya) that is invisible in panel b because of polarity reversal of the arrivals with backazimuth. (d) Interpretation and comparison with INDEPTH results; our relocated hypocenters are shown.

midcrustal layer is found and is interpreted as the decollement separating the Himalaya and the Indian plate. The decollement is invisible in the standard common conversion point stack of receiver functions, and a new method was developed to allow azimuthal difference stacks, making such anisotropic shear zones visible (Fig. 8c).

CONCLUSIONS

Results of the HIMNT experiment confirm and further detail the seismotectonics of the Himalayan collision zone. Over 1600 local earthquakes were recorded and located during the one-year experiment, and show upper crustal seismicity concentrated beneath the region with highest topographic relief of Nepal. A strongly bimodal distribution of seismicity is found beneath Tibet, with earthquakes concentrated in the upper crust and near the crust-mantle boundary, and a lower crust that is nearly aseismic. Seismic focal mechanisms show E–W extension in the upper crust beneath Tibet and predominantly strike-slip near the crust–mantle boundary. Crustal earthquakes beneath Nepal are mainly thrust and strike-slip. Teleseismic receiver functions find a strong Moho arrival corresponding to 45 km depth beneath Nepal and 75 km depth beneath Tibet. We find that the Moho is steepened but remains continuous beneath the Himalaya. Anisotropic receiver function imaging reveals seismic evidence for the decollement associated with the Main Himalayan Thrust.

ACKNOWLEDGEMENTS

We thank the Department of Mines and Geology of Nepal and the Chinese Academy of Science for their assistance with the HIMNT field project, and the IRIS consortium for providing seismic equipment. We thank John Nabelek and Wang-Ping Chen for their hospitality in Kathmandu. This work was supported by National Science Foundation Grants EAR 9903066 and EAR 0538259.

REFERENCES

Ammon, C. J., Randall, G. E., and *mtinv*, 1994, Deviatoric moment tensor inversion. http//:eqseis.geosc.psu.edu/~cammon/HTML/MTinvDocs/mtinv01.html, 2005.

Chen, W. P. and Yang, Z., 2004, Earthquakes beneath the Himalayas and Tibet: Evidence for Strong Lithospheric Mantle. Science, v. 304, pp. 1949–1952.

De la Torre, T. L. and Sheehan, A. F., 2005, Broadband seismic noise analysis of the Himalayan Nepal Tibet Seismic experiment. Bull. Seismol. Soc. Am., v. 95, 1202–1208, doi:10.1785/0120040098.

De la Torre, T. L., Monsalve, G. , Sheehan, A. F., Sapkota, S., and Wu, F., 2007, Earthquake processes of the Himalayan collision zone in eastern Nepal and the southern Tibetan Plateau. Geophys. Jour. Int., *in press*.

Eberhart-Phillips, D., 1986, Three-dimensional velocity structure in the Northern California Coast Ranges from inversion of local earthquake arrival times. Bull. Seismol. Soc. Am., v. 76, pp. 1025–1052.

Eberhart-Phillips, D., 1990, Three-dimensional P and S velocity structure in the Coalinga region, California. Jour. Geophys. Res., v. 95, pp. 15343–15363.

Eberhart-Phillips, D. and Michael, A. J., 1998, Seismotectonics of the Loma Prieta, California, region determined from three-dimensional Vp, Vp/Vs and seismicity. Jour. Geophys. Res., v. 103, pp. 21099–21120.

Husen, S., Kissling, E., and Flueh, E., 2000, Local earthquake tomography of shallow subduction in north Chile: A combined on-shore and off-shore study. Jour. Geophys. Res., v. 105, pp. 28183–28198.

Lavé, J. and Avouac, J. P., 2001, Fluvial incision and tectonic uplift across the Himalayas of central Nepal. Jour. of Geophysical Research-Solid Earth, v. 106 (B11), pp. 26561–26591.

Lomax, A., 2004, Probabilistic, Non-Linear, Global-Search earthquake location in 3D media. NonLinLoc Version 3.03, Anthony Lomax Scientific Software, Mouans-Sartoux, France.

Lyon-Caen, H. and Molnar, P. , 1983, Constraints on the Structure of the Himalaya from an Analysis of Gravity-Anomalies and a Flexural Model of the Lithosphere. Jour. of Geophysical Research, v. 88 (NB10), pp. 8171–8191.

Maggi, A., Jackson, J. A., McKenzie, D., and Priestley, K., 2000, Earthquake Focal Depths, Effective Elastic Thickness and the Strength of the Continental Lithosphere. Geology, v. 28, pp. 495–498.

Menke, W., 1989, *Geophysical data analysis: Discrete inverse theory.* Academic Press.

Michelini, A. and McEvilly, T.V., 1991, Seismological studies at Parkfield. I. Simultaneous inversion for velocity structure and hypocenters using cubic B-splines parameterization. Bull. Seismol. Soc. Am., v. 81, pp. 524–552.

Molnar, P. and Lyon-Caen, H., 1988, Fault plane solutions of earthquakes and active tectonics of the Tibetan Plateau and its margins. Geophysical Jour. Int., v. 99, p. 123–153.

Monsalve, G., Sheehan, A. F., Schulte-Pelkum, V. , Rajaure, S., Pandey, M. R., and Wu, F., 2006, Seismicity and one-dimensional velocity structure of the Himalayan collision zone: Earthquakes in the crust and upper mantle. Jour. Geophys. Res., v. 111, B10301, doi:10.1029/2005JB004062.

Nelson, K. D., Zhao, W., Brown, L. D., Kuo, J. , Che J., Liu, X., Klemperer, S. L., Makovsky, Y., Meissner, R., Mechie, Kind, J. R., Wenzel, F., Ni, J., Nabelek, J., Leshou Chen Handong Tan Wenbo Wei, Jones, A. G., Booker, J., Unsworth, M., Kidd, W. S. F. , Hauck, M., Alsdorf, D., Ross, A., Cogan, M., Wu, C., Sandvol, E., Edwards, M.,1996, Partially molten middle crust beneath southern Tibet; synthesis of Project INDEPTH results. Science, v. 274, n. 5293, pp. 1684–1688.

Pandey, M. R., Tandukar, R. P., Avouac, J. P., Lavé, J., and Massot, J. P., 1995, Interseismic strain accumulation on the Himalayan crustal ramp (Nepal). Geophys. Res. Lett., v. 22, pp.751–754.

Schulte-Pelkum, V., Monsalve, G., Sheehan, A., Pandey, M. R., Sapkota, S., Bilham, R., and Wu, F., 2005, Imaging the Indian subcontinent beneath the Himalaya. Nature, v. 435, pp. 1222–1225.

Thurber, C., 1983, Earthquake locations and three-dimensional crustal structure in the Coyote Lake area, Central California. Jour. Geophys. Res., v. 88, pp. 8226–8236.

Thurber, C., 1993, Local earthquake tomography: Velocities and Vp/Vs – Theory, in *Seismic Tomography: Theory and Practice*. Edited by: H. M. Iyer and K. Hirahara, pp. 563–583, Chapman and Hall, New York.

Toomey, D. R. and Foulger, G. R., 1989, Tomographic inversion of local earthquake data from the Hengill-Grensdalur central volcano complex, Iceland. Jour. Geophys. Res., v. 94, pp. 17497–17510.